Electronic Supplementary Material (ESI) for Journal of Materials Chemistry A.
This journal is © The Royal Society of Chemistry 2020

Supporting Information

Novel Highly Active and Self-Healing $Co(CO_3)_xOH_y$ Cocatalysts on $BiVO_4$ Photoanodes for Effective Solar Water Oxidation

Lijun Wu,[1] Lei Wang,[1,2,*] Jie Zhu,[1] Mao Sun,[1] Xianhu Liu,[2] Patrik Schmuki,[3,4,5,*] and Jun Zhang[1,*]

[1] School of Chemistry and Chemical Engineering & Inner Mongolia Engineering and Technology Research Center for Catalytic Conversion and Utilization of Carbon Resource Molecules, Inner Mongolia University, 235 West University Street, Hohhot 010021, P. R. China

E-mail: wanglei@imu.edu.cn; cejzhang@imu.edu.cn

[2] Key Laboratory of Materials Processing and Mold, Ministry of Education, Zhengzhou University, Zhengzhou 450002, P.R. China

[3] Department of Materials Science and Engineering WW4-LKO, University of Erlangen-Nuremberg, Martensstrasse 7, D-91058 Erlangen, Germany.

E-mail: schmuki@ww.uni-erlangen.de

[4] Regional Centre of Advanced Technologies and Materials, Faculty of Science, Palacky University, Olomouc, Šlechtitelů 27, 783 71 Olomouc, Czech Republic

[5] Chemistry Department, Faculty of Sciences, King Abdulaziz University, 80203 Jeddah, Saudi Arabia Kingdom

Experimental Section

1. *Preparation of $BiVO_4$, $BiVO_4/Co(CO_3)_xOH_y$, $BiVO_4$@Co, $BiVO_4$@Urea, $BiVO_4/Co_3O_4$, $BiVO_4$/CoOOH, $BiVO_4$/Co-Pi photoanodes.*

Before the synthesis, the fluorine-doped tin oxide (FTO) was sonicated in acetone, ethanol and water for 15 minutes. Wrap the FTO with Kapton tape to ensure an effective area of 1 cm^2. Preparation of nanoporous $BiVO_4$ is according to a literature procedure.[1] First, the BiOI film was electrodeposited on FTO, and then this film was converted into $BiVO_4$ film. In detail, 50 mL of 0.4 M KI solution was prepared, and after stirring for 10 minutes, concentrated HNO_3 was added to adjust the pH to 1.7. The 0.04 M $Bi(NO_3)_3{\cdot}5H_2O$ was then added to the above solution, and after stirring for 15 minutes, 20 mL of a 0.23 M p-benzoquinone ethanol solution was added. A typical three-electrode cell is used for electrodeposition of BiOI films. The deposition of the BiOI film was carried out at -0.1 V vs Ag/AgCl for 5 minutes at room temperature. 150 μL of a DMSO solution containing 0.2 M vanadyl acetylacetonate ($VO(acac)_2$) was placed on a BiOI film, and the precursor was heated in a muffle furnace at 450 °C for 2 h in air. After cooling to room temperature, the resulting electrode was immersed in a 1 M NaOH solution for 40 minutes with mild stirring to remove excess V_2O_5. Finally, the obtained pure mesoporous $BiVO_4$ electrode is rinsed with deionized water and dried in air.

For the $BiVO_4/Co(CO_3)_xOH_y$, the precursor solution containing 6 mM $Co(NO_3)_2{\cdot}6H_2O$ and 30 mM urea was under vigorous stirring, a piece of $BiVO_4$/FTO was put in the autoclave. 36 mL precursor solution was transferred to a 50 mL Teflon-lined stainless steel autoclave and held at 120 °C for 12 h. The synthetic procedure of $BiVO_4$@Co or $BiVO_4$@Urea is the same as above except for only addition of $Co(NO_3)_2{\cdot}6H_2O$ or Urea, respectively. The $BiVO_4/Co_3O_4$ photoanode was prepared by annealing $BiVO_4/Co(CO_3)_xOH_y$ at 400 °C for 2 h in air. The $BiVO_4$/CoOOH photoanode was prepared by a solution impregnation.[2] A piece of $BiVO_4$/FTO was immersed in a mixed solution of 0.1 M $Co(NO_3)_2{\cdot}6H_2O$ and 0.1 M NaOH with a ratio of 1:1 for 30 min. The $BiVO_4$/Co-Pi photoanode is synthesized by an

electrochemical deposition.[3] The $BiVO_4$ photoanode was held potentiostatically at 1.0 V vs. Ag/AgCl for 1 min in a solution containing 0.5 mM $Co(NO_3)_2 \cdot 6H_2O$ and 0.1 M KH_2PO_4 (pH=7).

2. Preparation of $BiVO_4$/FeOOH, $BiVO_4$/NiOOH photoanodes.

The synthesis of $BiVO_4$/FeOOH and $BiVO_4$/NiOOH photoanodes by a photo-assisted electrodeposition process under AM 1.5G illumination was modified according to previous report.[1] Electrodeposition of FeOOH on the $BiVO_4$ electrodes was carried out in a 0.1 M $Fe(SO_4)_2 \cdot 7H_2O$ solution previously purged with N_2 for 20 min at an external bias of ca. 0.25 V vs. Ag/AgCl for 15 min. NiOOH was deposited from a 0.1 M $Ni(SO_4)_2 \cdot 6H_2O$ solution at 0.11 V vs. Ag/AgCl for 5 min. For both co-catalysts, after photodeposition, additional electrodeposition was carried out in the same solution by applying 1.2 V vs. Ag/AgCl for 1 min in the dark to deposit FeOOH or NiOOH on any bare $BiVO_4$ surfaces.

3. Preparation of $Co(CO_3)_xOH_y$/NF, CoOOH/NF, Co-Pi/NF, Co_3O_4/NF electrocatalysts.

The preparation of $Co(CO_3)_xOH_y$/NF, CoOOH/NF, Co-Pi/NF and Co_3O_4/NF electrocatalysts is same to the preparation of $BiVO_4/Co(CO_3)_xOH_y$, $BiVO_4$/CoOOH, $BiVO_4$/Co-Pi and $BiVO_4/Co_3O_4$, except that $BiVO_4$/FTO is replaced by treated NF.

4. *Photoelectrochemical measurements.*

The photoelectrochemical properties were measured by an electrochemical analyzer (CHI760D, CH Instruments, Inc.) in a standard three-electrode system. The illumination source was a simulated sunlight AM 1.5G (100 mW/cm^2, PLS-FX300HU, Beijing Perfectlight Technology Co., Ltd.), and a 1 M potassium borate aqueous solution (KBi, pH=9.5) was used as the electrolyte. Photocurrent vs. voltage (*J*-*V*) characteristics were recorded by scanning the potential from -0.6 to 0.6 V (vs. Ag/AgCl) with a scan rate of 10 mV s^{-1}. The measured potentials vs. Ag/AgCl were converted to the reversible hydrogen electrode (RHE) scale. The incident photon to current efficiency (IPCE) was determined using amonichromatic light by a Xe lamp (CEL-SLF-Vertex, CEAULIGHT Co., China). IPCE was

measured at 1.23 V_{RHE} in 1 M KBi. Electrochemical impedance spectroscopy (EIS) Nyquist plots were taken at 0.6 V_{RHE} with small AC amplitude of 10 mV in the frequency range of 10^{-2} to 10^5 Hz in the light. Oxygen and hydrogen evolution were collected in an air-tight cell at 1.23 V_{RHE} under AM 1.5 illumination. The amount of gases was measured with a gas chromatograph (Shimadzu, GC-2014C) every 30 min. The surface charge injection efficiency ($\eta_{surface}$) was calculated using the equation:

$$\eta_{surface} = (J_{water}/J_{sulfite})\times 100 \qquad (1)$$

where J_{water} was the current density acquired in the 1 M KBi without Na_2SO_3, $J_{sulfite}$ was the current density acquired in the presence of 0.2 M Na_2SO_3 in 1 M KBi. The charge separation efficiency ($\eta_{abs}\times\eta_{sep}$) can be calculated using the following equation:

$$\eta_{abs}\times\eta_{sep} = (J_{water}/J_{abs})\times 100 \qquad (2)$$

where j_{abs} was the theoretical current density assuming the complete conversion of the absorbed irradiation.

5. Materials characterization.

The crystalline structure was identified by X-ray diffraction analysis (Rigaku RINT-2000) using Cu Kα radiation at 40 kV and 40 mA. The elemental composition was determined by X-ray photoelectron spectroscopy (ESCALABXI+). Scanning electron microscopy and transmission electron microscopy were carried out using Hitachi S-4800 system and FEI Tecnai TF20 microscope for morphology observation. UV-visible diffuse reflectance spectra were performed on a UV-2550 (Shimadzu) spectrometer by using $BaSO_4$ as the reference. Raman spectroscopy characterizations were carried out using a Renishaw Invia Raman microscope with a 532 nm laser source under vacuum conditions in an in–situ reaction cell. Fourier transform infrared spectra of the samples were recorded on a PerkinElmer IR spectrometer by using KBr as the reference. The inductively coupled plasma-mass spectrometry was conducted in Nexion 300 machine.

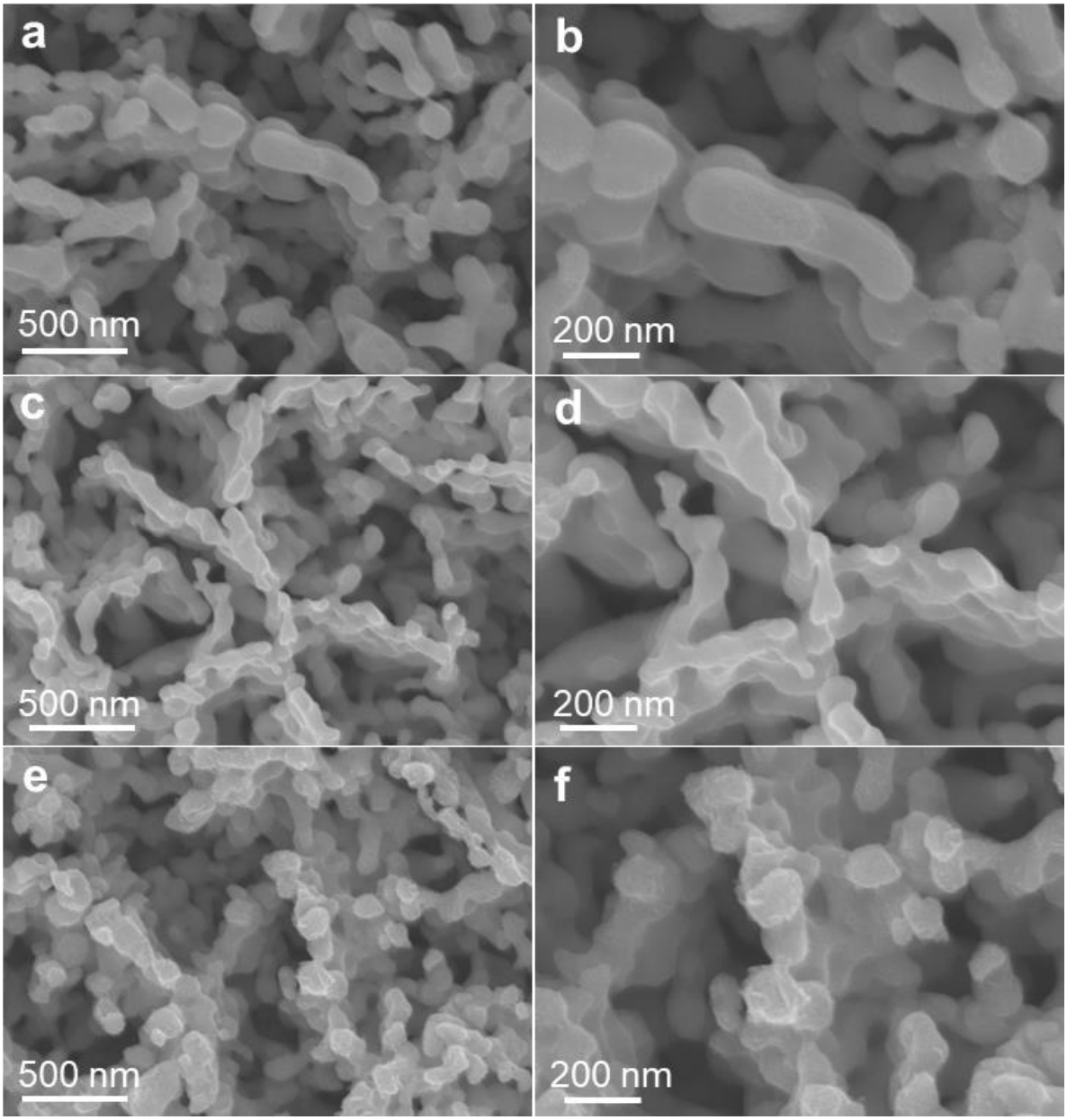

Figure S1. SEM images of (a,b) BVO, (c,d) BVO/$Co(CO_3)_xOH_y$, and (e,f) BVO/CoOOH.

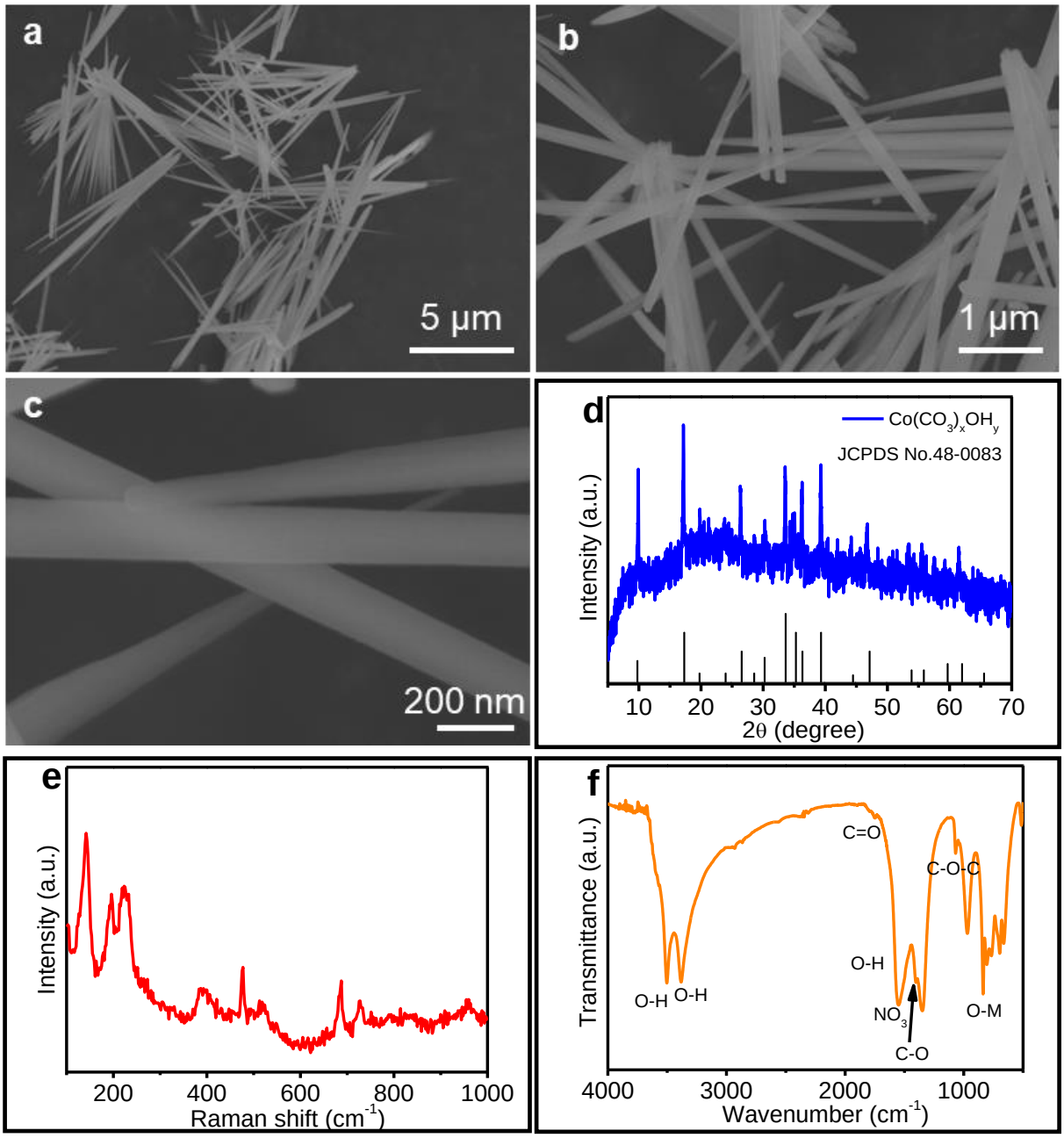

Figure S2. (a-c) SEM images, (d) XRD pattern, (e) Raman spectrum, and (f) FTIR spectrum of $Co(CO_3)_xOH_y$.

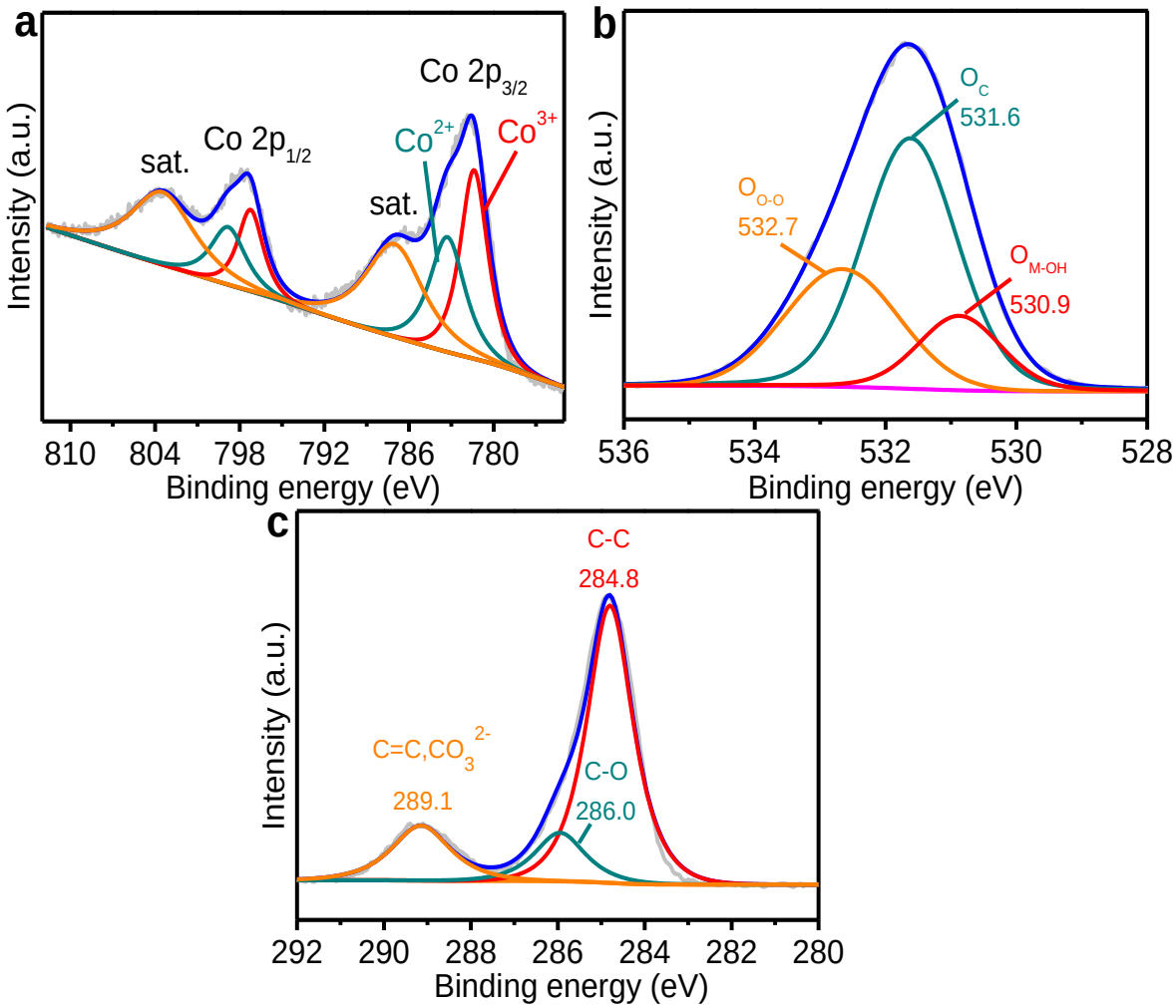

Figure S3. XPS high resolution (a) Co 2p, (b) O 1s, and (c) C 1s spectra of $Co(CO_3)_xOH_y$.

In the O 1s spectrum (**Figure S3b**), O 1s is fitted into three peaks centered at 530.9 eV, 531.6 eV, and 532.7 eV, which are attributed to hydroxyl groups ($O_{M\text{-}OH}$), carbonate species (O_C) and a chemisorbed or dissociated oxygen species from water molecules ($O_{O\text{-}O}$), respectively.[4] Moreover, in the C 1s spectrum (**Figure S3c**), three peaks at 284.8 eV, 286.0 eV, and 289.1 eV can be assigned to the C-C, C-O, and CO_3^{2-} bonds, respectively.

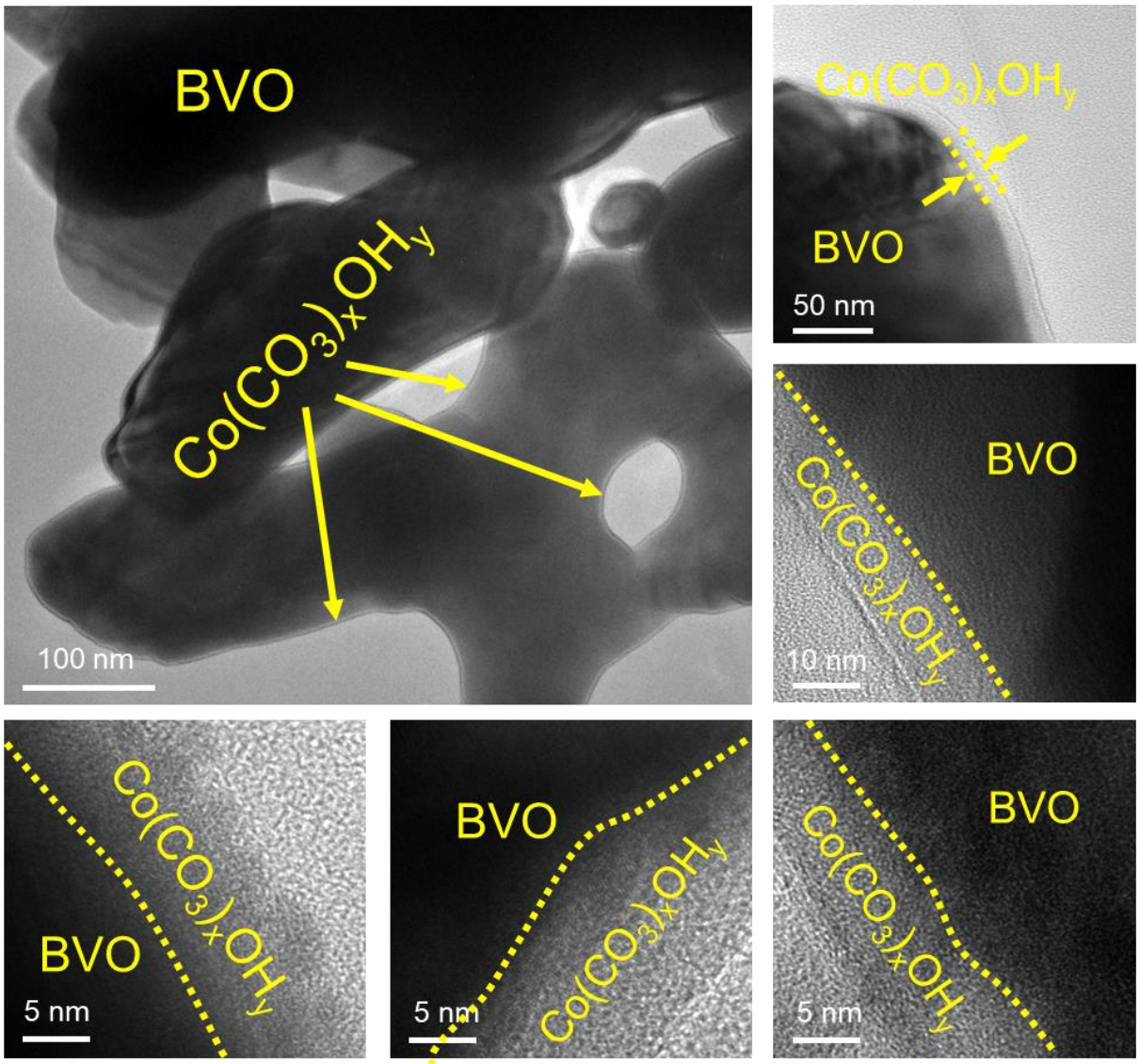

Figure S4. TEM images of BVO/$Co(CO_3)_xOH_y$.

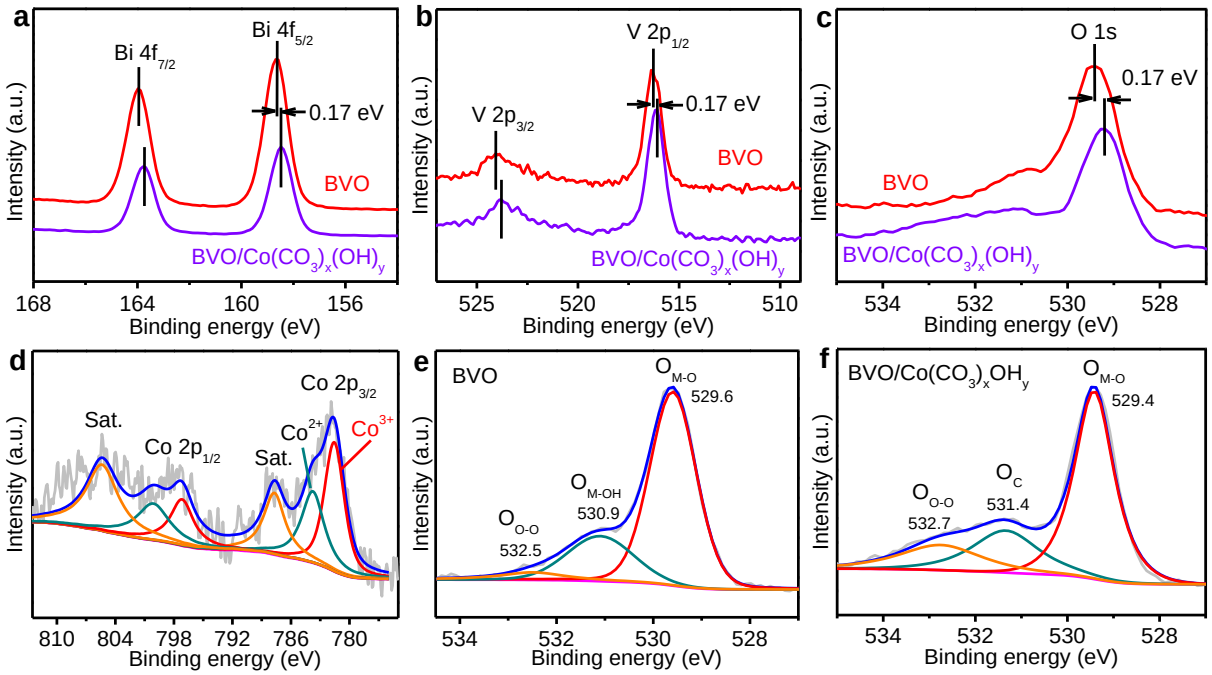

Figure S5. (a-c) XPS high resolution (a) Bi 4f, (b) V 2p, and (c) O 1s spectra of BVO and BVO/$Co(CO_3)_xOH_y$; (d) curve fits of Co 2p peak of BVO/$Co(CO_3)_xOH_y$; (e,f) curve fits of O 1s peaks of (e) BVO and (f) BVO/$Co(CO_3)_xOH_y$.

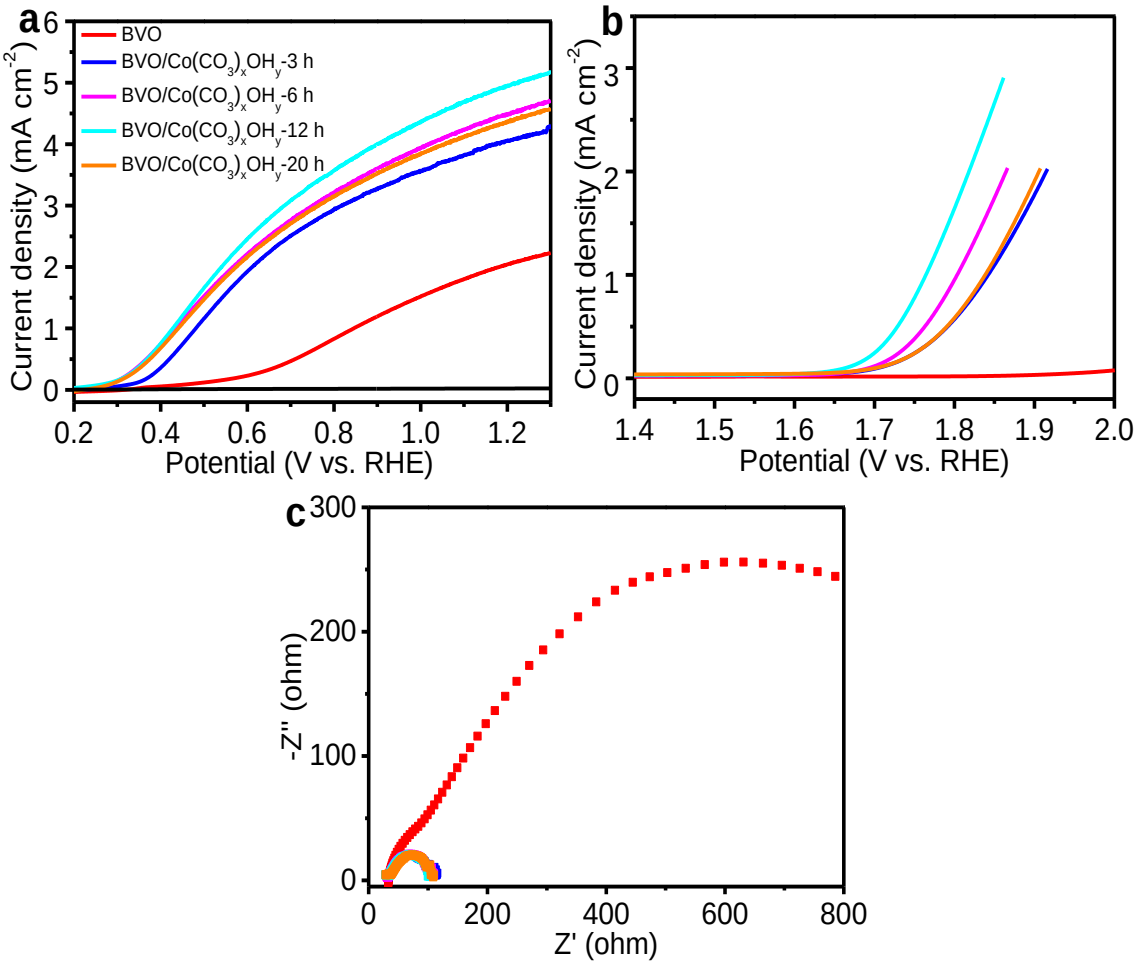

Figure S6. (a,b) LSV curves in light (a) and dark (b), and (c) EIS spectra at 0.6 V_{RHE} of $BVO/Co(CO_3)_xOH_y$ with different hydrothermal times in 1 M KBi.

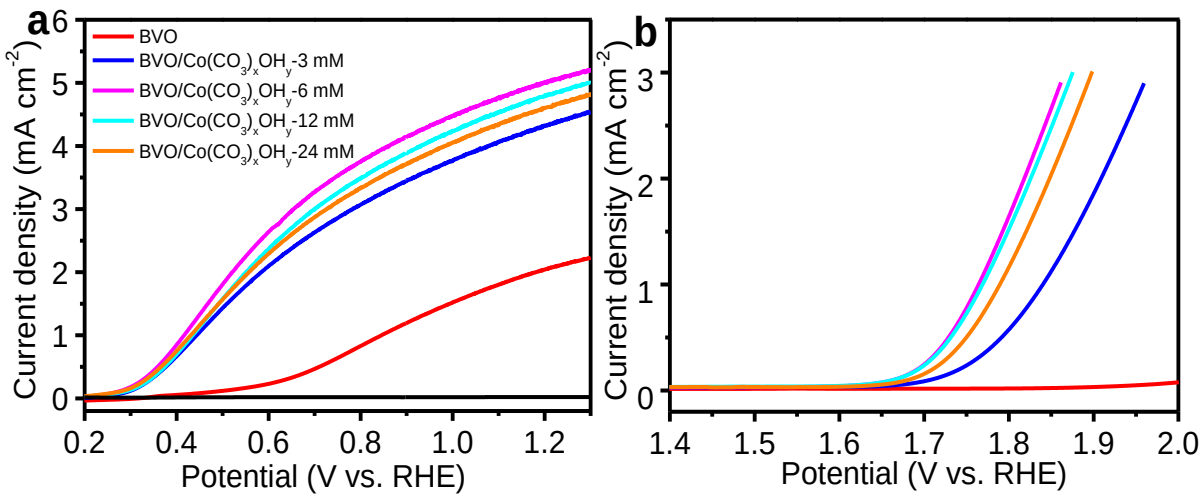

Figure S7. LSV curves of BVO/$Co(CO_3)_xOH_y$ with different $Co(NO_3)_3$ concentrations in 1 M KBi (a) under AM 1.5G (100 mW cm^{-2}) and (b) in dark.

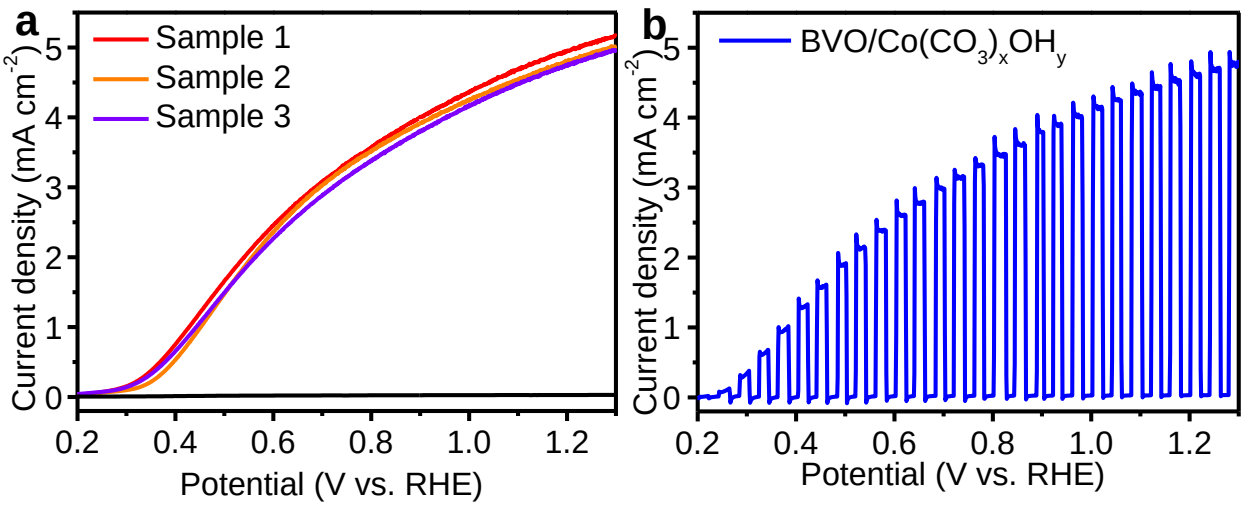

Figure S8. (a) Reproductivity of LSV curves, and (b) chopped light of LSV curve of $BVO/Co(CO_3)_xOH_y$ under AM 1.5G (100 mW cm^{-2}) in 1 M KBi.

Table S1. Comparison of PEC activities for BVO photoanodes with the modification of Co-based OECs.

Photoanodes	*J* @ 1.23 V_{RHE}	Electrolyte	References
Co-Pi/etched p-BVO	6.1 mA cm^{-2}	0.5 M phosphate buffer (pH 7)	Energy Environ. Sci. 2018, 11, 1299.
Co-Pi/gradient-doped W:BVO	3.6 mA cm^{-2}	0.1 M phosphate buffer (pH 7.3)	Nat. Commun. 2013, 4, 2195.
CoBi/electrochemically treated BVO	3.2 mA cm^{-2}	0.5 M phosphate borate (pH 9.5)	Angew. Chem. Int. Ed. 2017, 56, 8500.
CoOOH/BVO	4.0 mA cm^{-2}	0.2 M potassium phosphate (pH 7)	ACS Appl. Mater. Interfaces 2018, 10, 6228.
Co-Pi/BVO	2.0 mA cm^{-2}	0.1 M potassium phosphate (pH 6.7).	Adv. Funct. Mater. 2016, 26, 4951.
Mo:$BiVO_4$/Co:$BiVO_4$	2.09 mA cm^{-2}	0.1 M potassium phosphate (pH 7)	Appl. Catal. B 2017, 211, 258.
Co-Pi/Mo:meso-BVO	4.57 mA cm^{-2}	0.1 M potassium phosphate (pH 7)	Appl. Catal. B 2018, 238, 586.
$LaCo(OH)_x/BiVO_4$	2.02 mA cm^{-2}	0.5 M potassium phosphate (pH 7)	ACS Energy Lett. 2017, 2, 1062.
$FeCoO_x/BiVO_4$	4.82 mA cm^{-2}	1 M potassium borate (pH 9.5).	Adv. Funct. Mater. 2018, 28, 1802685.
CoFe-H/$BiVO_4$	2.48 mA cm^{-2}	0.5 M potassium phosphate (pH 7)	Adv. Funct. Mater. 2017, 27, 1603904.
$Co_4O_4/BiVO_4$	5.0 mA cm^{-2}	0.5 M potassium borate buffer (pH 9.3)	Angew. Chem. Int. Ed. 2017, 56,6911.
$Co_3O_4/BiVO_4$	2.71 mA cm^{-2}	0.5 M potassium phosphate (pH 7)	J. Am. Chem. Soc. 2015, 137, 8356.
NiO/$CoO_x/BiVO_4$	3.5 mA cm^{-2}	0.1 M potassium phosphate (pH 7)	J. Am. Chem. Soc. 2015, 137, 5053.
Co-Pi@$BiVO_4/WO_3$	1.8 mA cm^{-2}	0.1 M potassium phosphate (pH 7)	ACS Appl. Mater. Interfaces 2019, 11, 5623.
$Co(CO_3)_xOH_y$/BVO	**5.0 mA cm^{-2}**	**1 M KBi (pH 9.5)**	**In this work.**

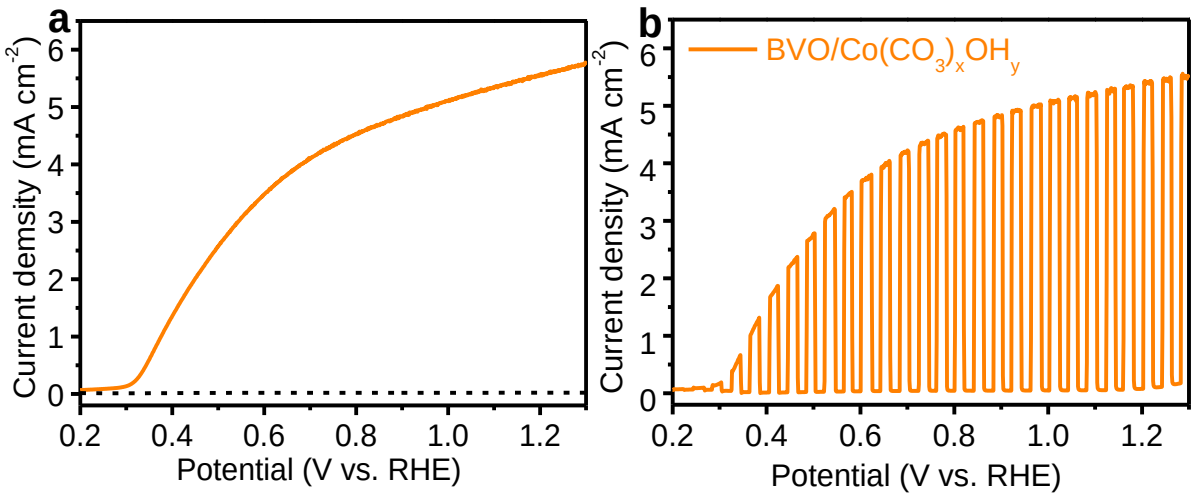

Figure S9. (a) LSV curve and (b) chopped light of BVO/$Co(CO_3)_xOH_y$ under 1.5G (100 mW cm^{-2}) illumination in 1 M KBi+Na_2SO_3.

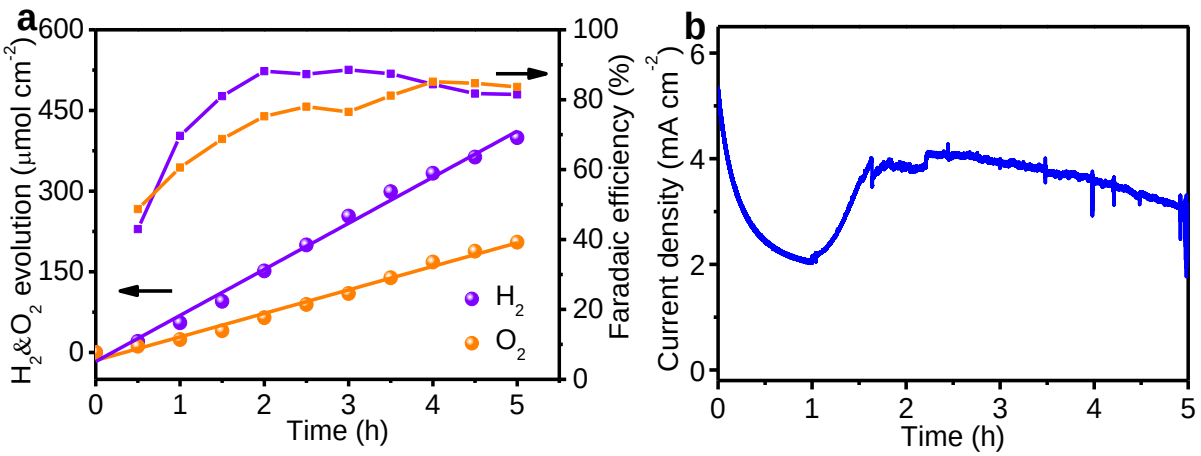

Figure S10. (a) Oxygen and hydrogen evolution detected by gas chromatography and faradaic efficiency, and (b) *i-t* curve of BVO/$Co(CO_3)_xOH_y$ at 1.23 V_{RHE} for 5 h under AM 1.5G (100 mW cm^{-2}) in 1 M KBi.

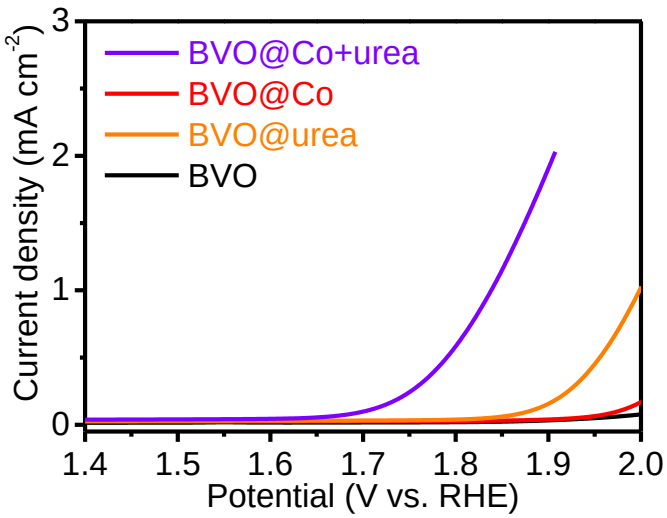

Figure S11. LSV curves of BVO photoanodes in different hydrothermal conditions in dark.

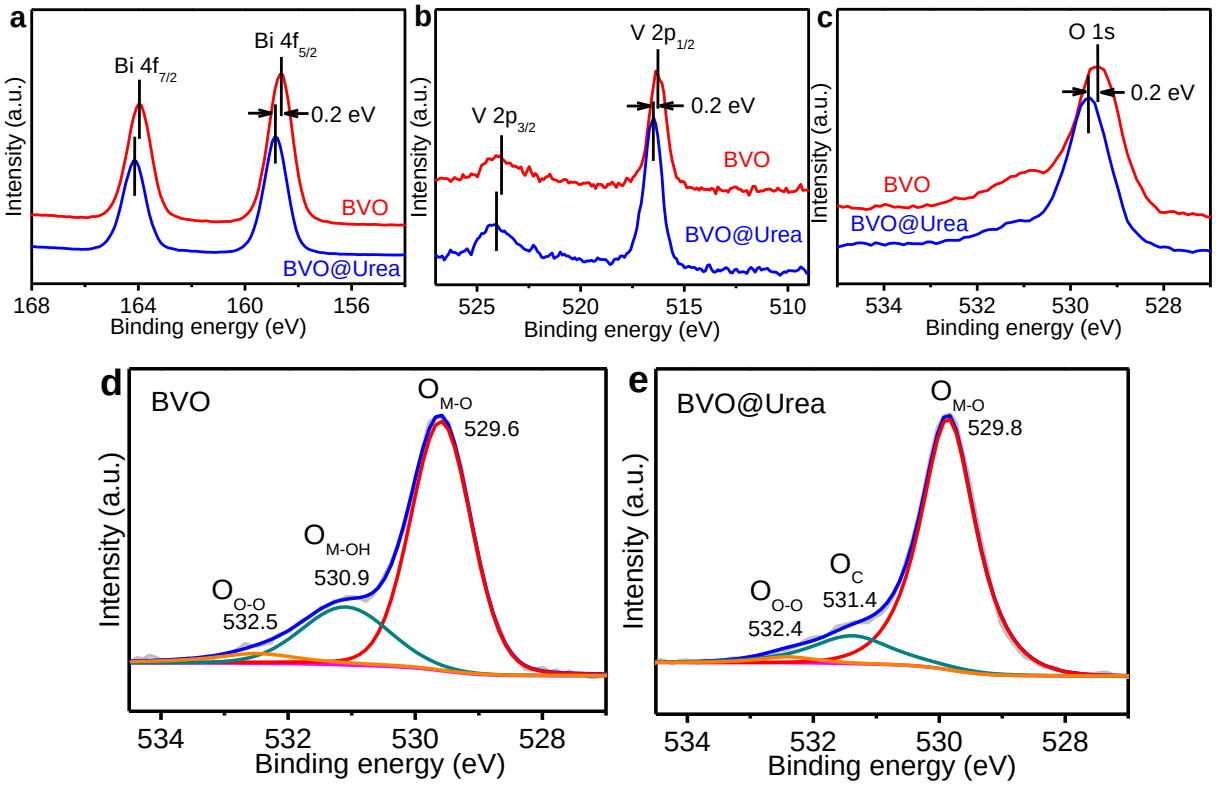

Figure S12. (a-c) XPS high resolution (a) Bi 4f, (b) V 2p, and (c) O 1s spectra of BVO and BVO@urea; (d,e) curve fits of O 1s peaks of (d) BVO and (e) BVO@urea.

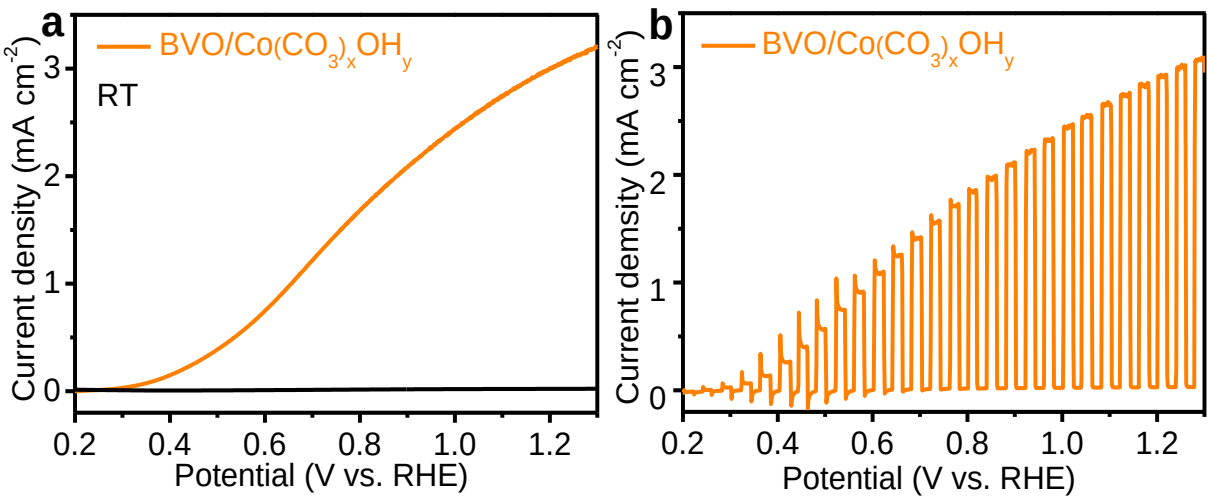

Figure S13. (a) LSV curve and (b) chopped light of BVO/$Co(CO_3)_xOH_y$ at room temperature under 1.5G (100 $mWcm^{-2}$) illumination in 1 M KBi.

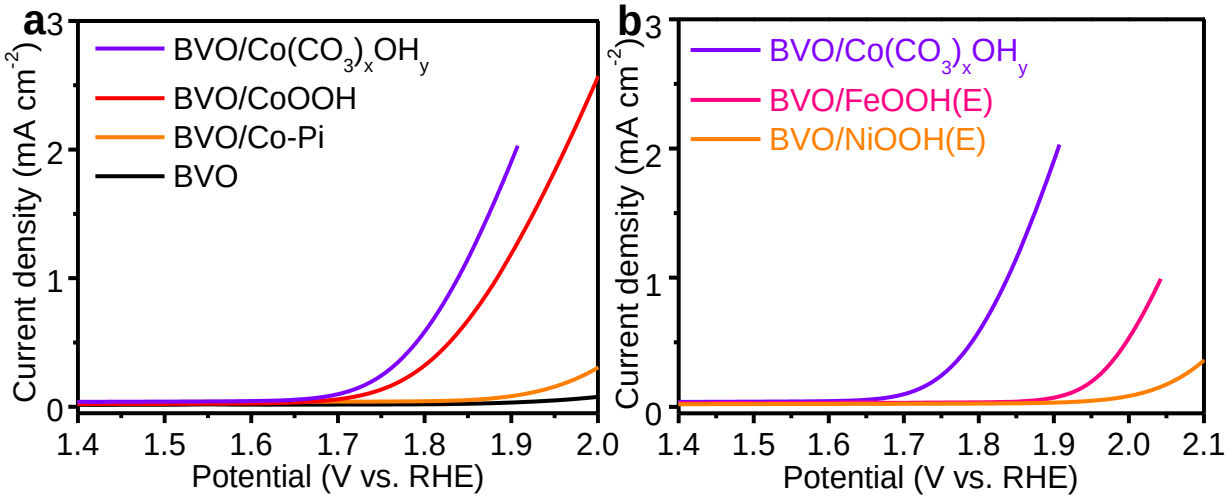

Figure S14. LSV curves of BVO, BVO/Co$(CO_3)_xOH_y$, BVO/CoOOH, and BVO/Co-Pi in 1 M KBi.

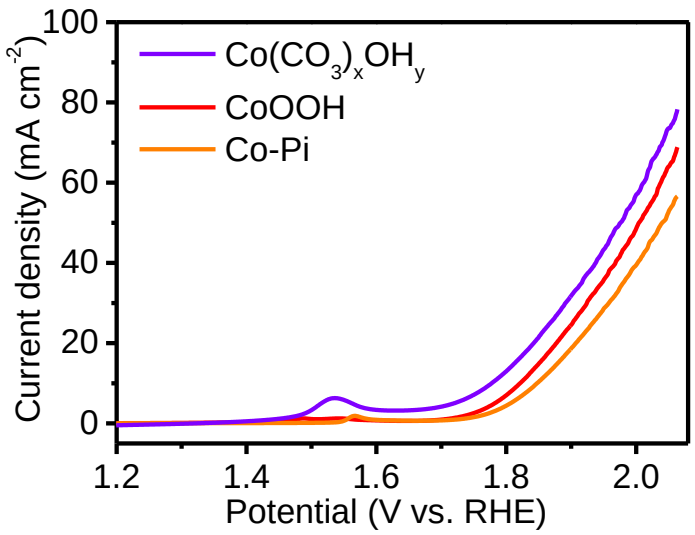

Figure S15. LSV curves of $Co(CO_3)_xOH_y$, CoOOH, and Co-Pi grown on nickel foams in 1 M KBi.

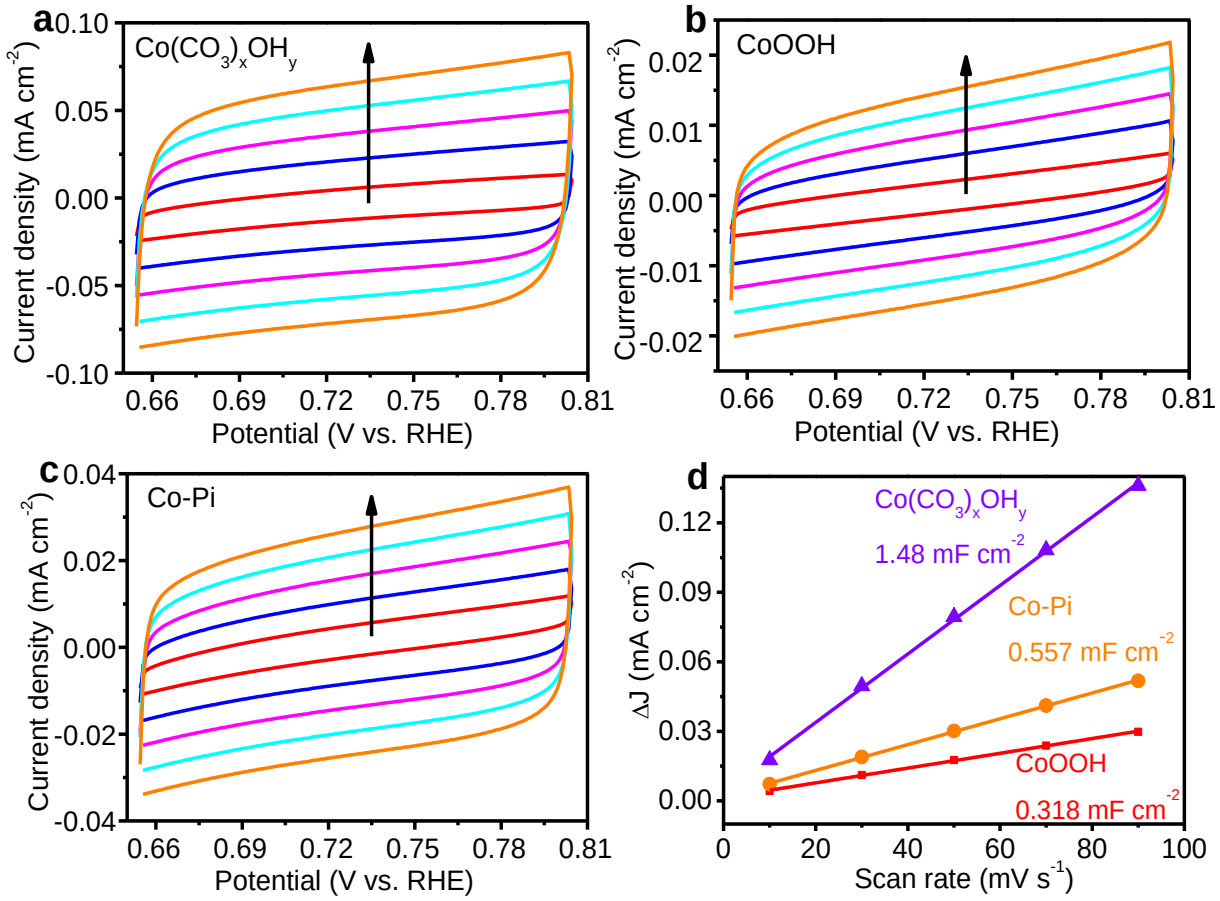

Figure S16. (a-c) Cyclic voltammetry curves, and (d) electrochemical surface areas of $Co(CO_3)_xOH_y$, CoOOH, and Co-Pi grown on nickel foams in 1 M KBi.

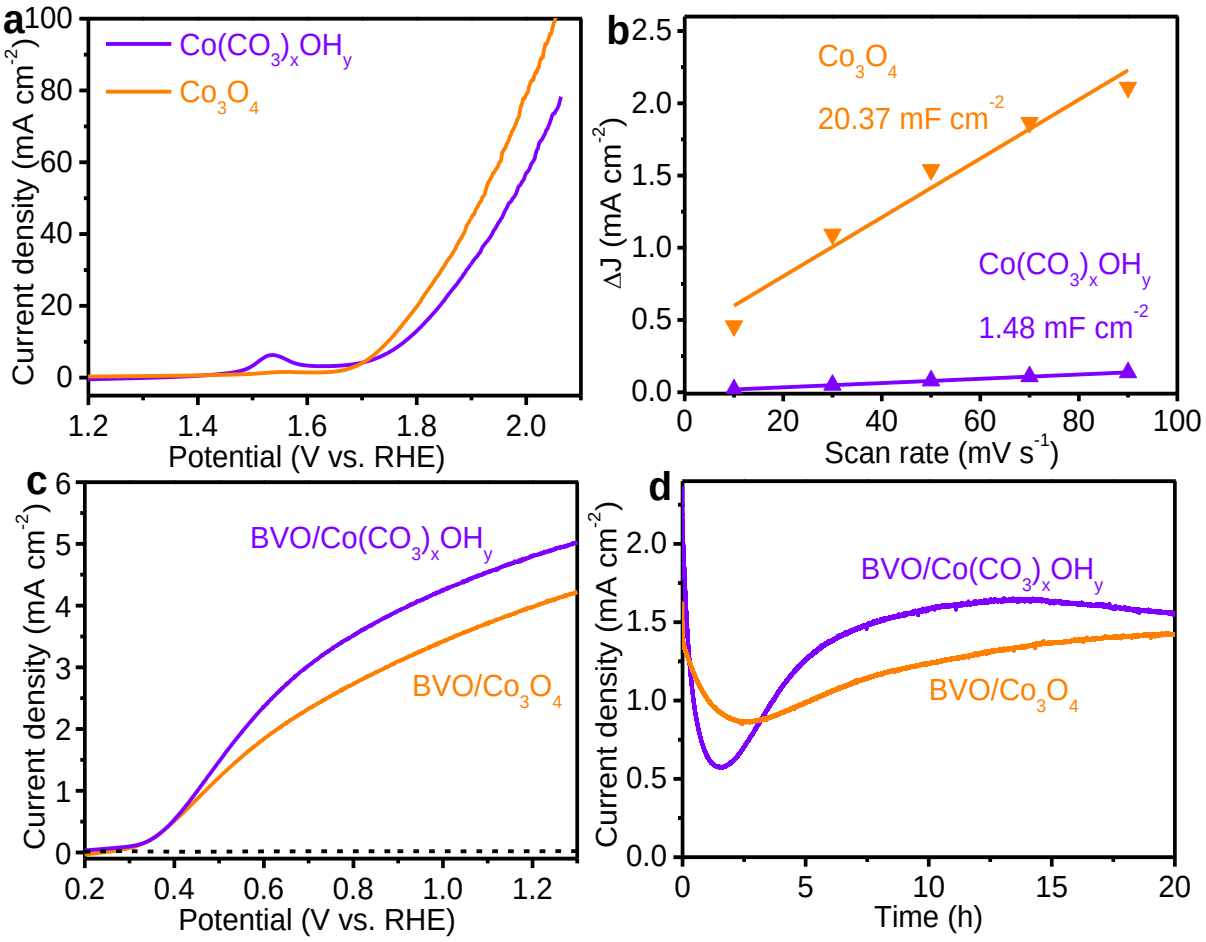

Figure S17. (a) LSV curves, and (b) electrochemical surface areas of Co_3O_4 grown on nickel foams in 1 M KBi; (c) LSV curves and (d) stability of BVO/Co_3O_4 under 1.5G(100 mW cm^{-2}) illumination in 1 M KBi. For the formation of Co_3O_4, BVO/$Co(CO_3)_xOH_y$ or $Co(CO_3)_xOH_y$/NF was annealed in air at 400 °C for 2 h.

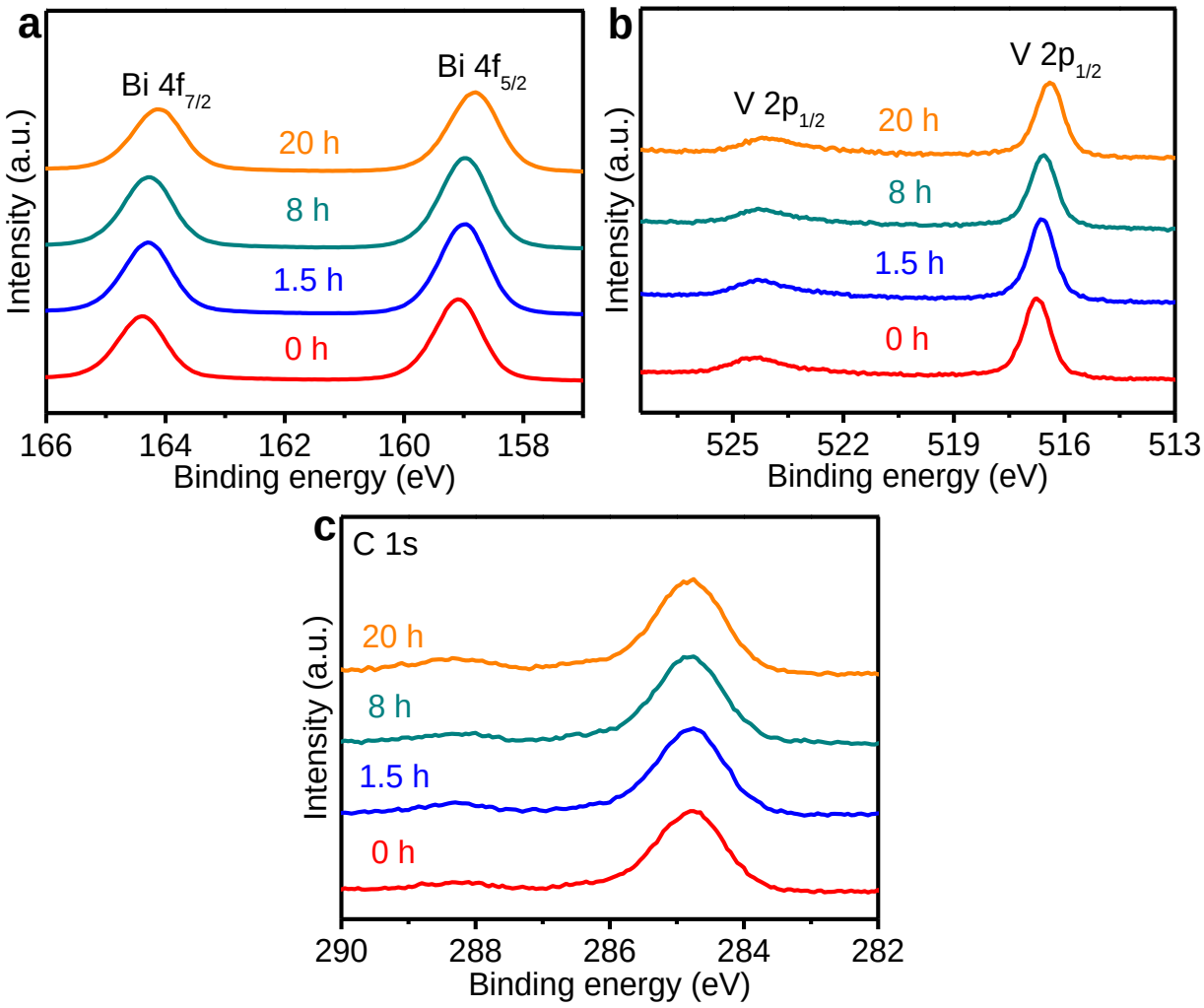

Figure S18. XPS high resolution (a) Bi 4f, (b) V 2p, and (c) C 1s spectra of BVO/$Co(CO_3)_xOH_y$ for various irradiation times in 1 M KBi.

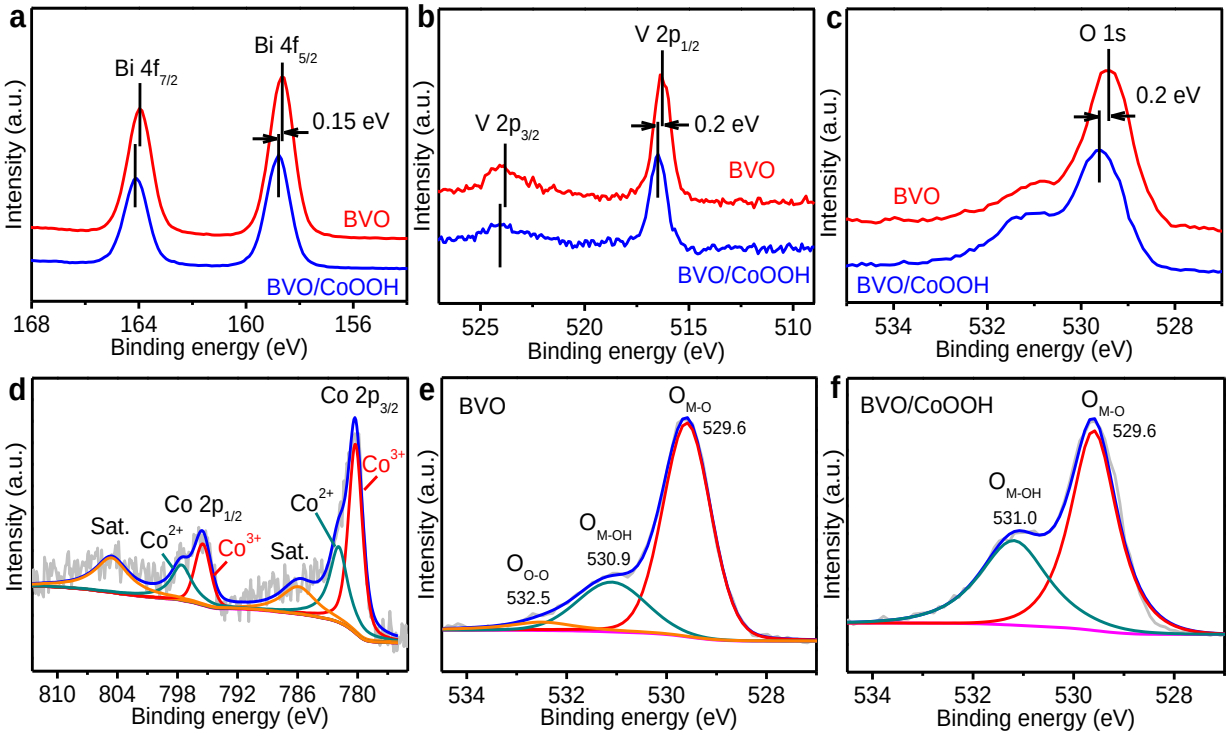

Figure S19. (a-c) XPS high resolution (a) Bi 4f, (b) V 2p, and (c) O 1s spectra of BVO and BVO/CoOOH; (d) curve fits of Co 2p peak of BVO/CoOOH; (e,f) curve fits of O 1s peaks of (e) BVO and (f) BVO/CoOOH.

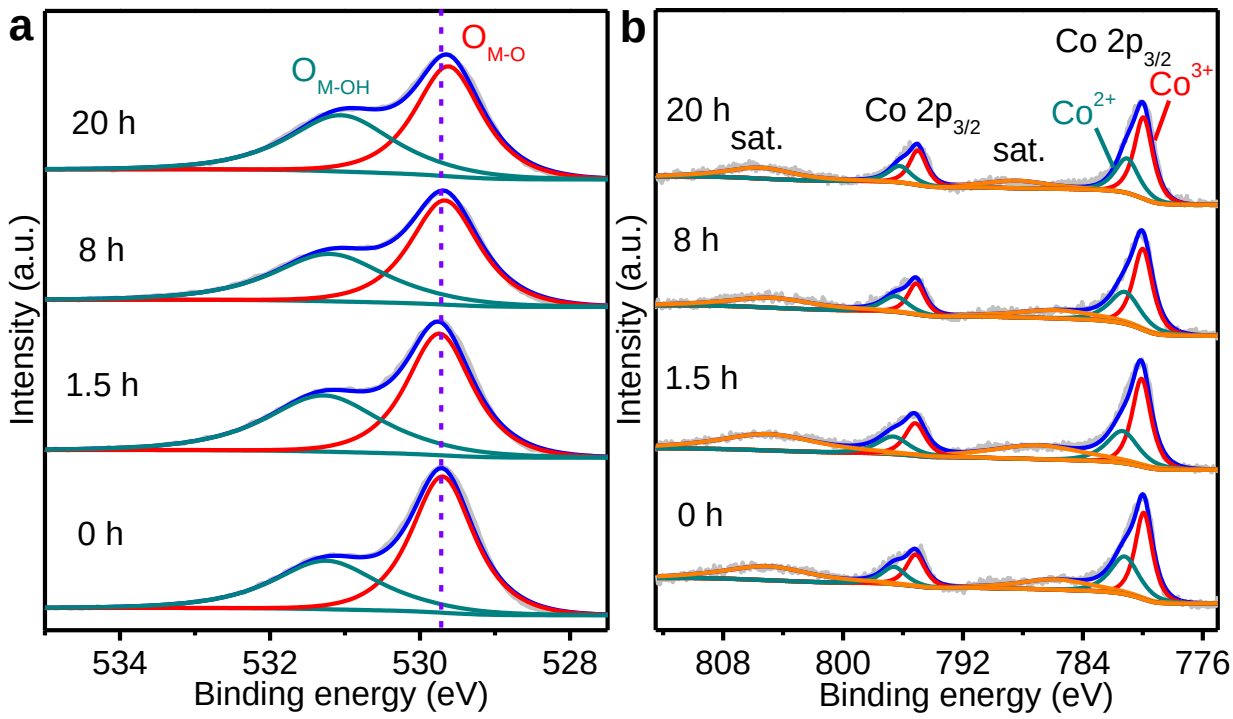

Figure S20. (a) O 1s and (b) Co 2p XPS spectra of BVO/CoOOH at 0.6 V_{RHE} under AM 1.5G (100 mW cm^{-2}) illumination with various times.

For comparison, the XPS spectra of BVO/CoOOH with different irradiation times was conducted (**Figure S19 and S20**). From **Figure S20**, the O 1s spectra show the similar metal-oxygen bond (M-O) and hydroxyl groups (O-H) in whole process.

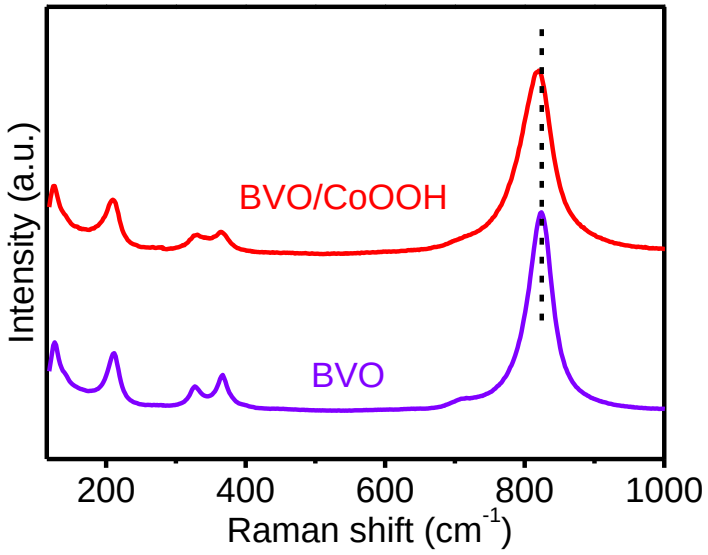

Figure S21. Raman spectra of BVO and BVO/CoOOH.

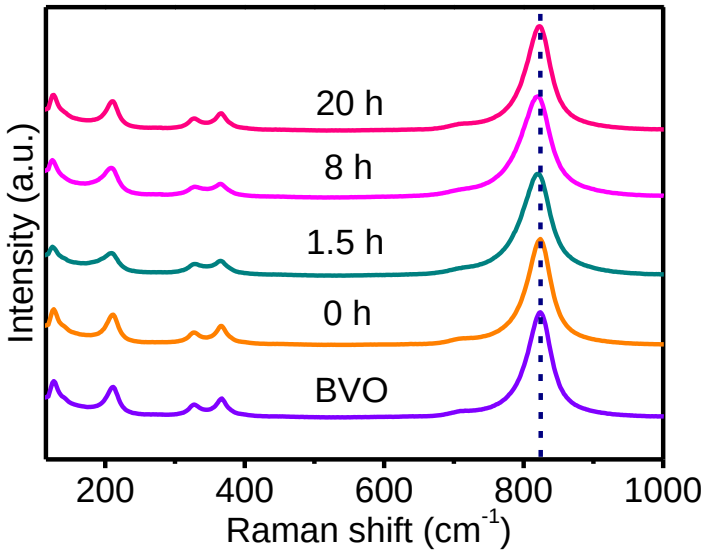

Figure S22. Raman spectra of BVO/$Co(CO_3)_xOH_y$ for various irradiation times in 1 M KBi.

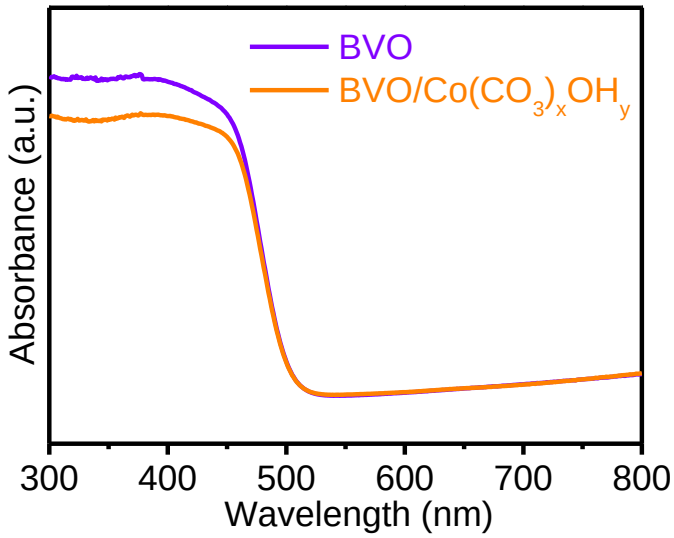

Figure 23. UV-vis spectra of BVO and BVO/$Co(CO_3)_xOH_y$.

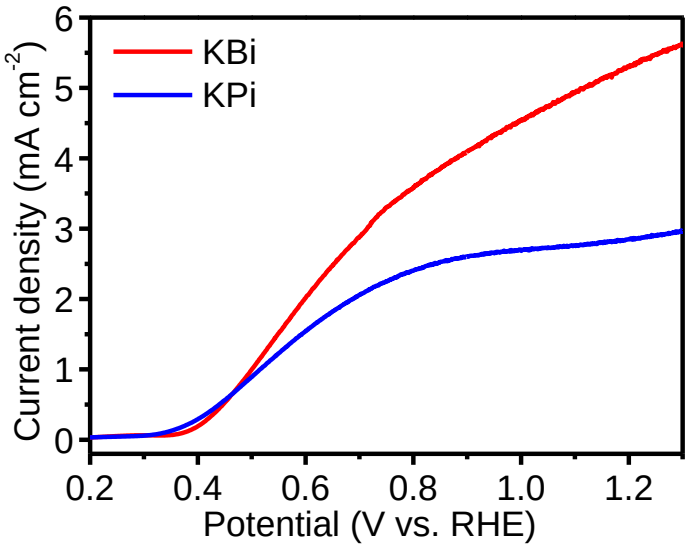

Figure 24. LSV curves of BVO/$Co(CO_3)_xOH_y$ in 1 M potassium borate buffer (KBi) and 1 M potassium phosphate buffer (KPi).

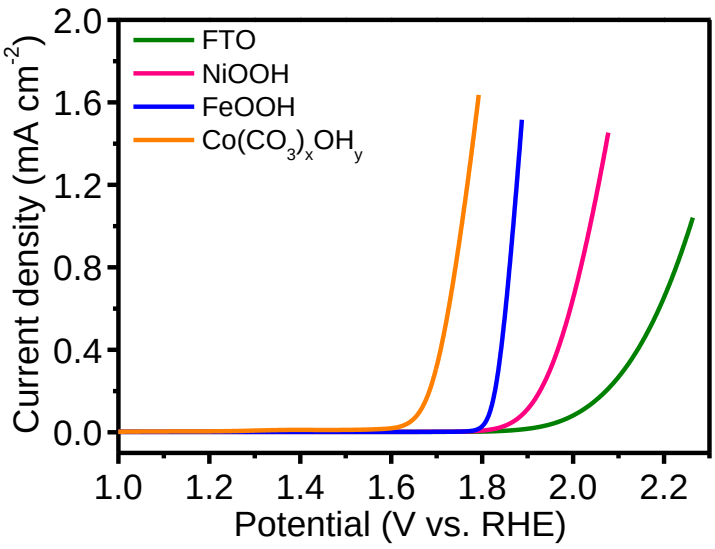

Figure 25. LSV curves of $Co(CO_3)_xOH_y$, FeOOH, and NiOOH grown on FTO substrates in 1 M KBi. FeOOH and NiOOH were prepared according to literature reported.[1]

References

1 T. W. Kim, K.-S. Choi, Science **2014**, 343, 990-994.

2. L. Wang, F. Dionigi, N. T. Nguyen, R. Kirchgeorg, M. Gliech, S. Grigorescu, P. Strasser, P. Schmuki, Chem. Mater. **2015**, 27, 2360-2366.

3. B. Zhang, L Wang, Y. Zhang, Y. Ding, Y. Bi, Angew. Chem. Int. Ed. **2018**, 57, 2248-2252.

4. J. Stoch, J. Gablankowska-Kukucz. Surf. Interface Analysis **1991**, 17, 165-167.